energies

MDPI

Article

Characteristic Evaluation of Different Carbonization Processes for Hydrochar, Torrefied Char, and Biochar Produced from Cattle Manure

Eunhye Song [1], Ho Kim [1], Kyung Woo Kim [1] and Young-Man Yoon [2,3,*]

[1] Bio Resource Center, Institute for Advanced Engineering, Yongin 17180, Republic of Korea; ehsong@iae.re.kr (E.S.); hokim0505@gmail.com (H.K.); fdc0726@iae.re.kr (K.W.K.)
[2] Biogas Research Center, Hankyong National University, Anseong 17579, Republic of Korea
[3] Plant Engineering Center, Institute for Advanced Engineering, Yongin 17528, Republic of Korea
* Correspondence: yyman@hknu.ac.kr

Abstract: The amount of cattle manure generated accounts for over 40% of the livestock manure in South Korea. Most livestock manure is utilized as a fertilizer and a soil amendment. However, the soil nutrients have exceeded saturation in South Korea. Accordingly, cattle manure, including lignocellulosic biomass, was applied for solid fuel production in this study. The three different types of carbonization process, namely, hydrothermal carbonization, torrefaction, and carbonization (slow pyrolysis), were estimated for a comparison of the hydrochar, torrefied char, and biochar characteristics derived from cattle manure. The processes were performed at temperatures ranging from 190 to 450 °C. The evaluation of the hydrochar, torrefied char, and biochar produced by three processes was conducted by the proximate, ultimate, calorific value, fuel ratio, and energy yield, which were used for the analysis of fuel quality. Additionally, the ash properties, including silicon dioxide, chlorine, and base-to-acid ratio (B/A) on hydrochar, torrefied char, and biochar were investigated to predict ash deposition during combustion. These analyses are essential to stabilize the operation of the combustion chamber. The thermogravimetric analysis represented the upgraded quality of hydrochar, torrefied char, and biochar by three different carbonization processes.

Keywords: cattle manure; hydrochar; torrefied char; biochar; hydrothermal carbonization; torrefaction; slow pyrolysis

Citation: Song, E.; Kim, H.; Kim, K.W.; Yoon, Y.-M. Characteristic Evaluation of Different Carbonization Processes for Hydrochar, Torrefied Char, and Biochar Produced from Cattle Manure. *Energies* **2023**, *16*, 3265. https://doi.org/10.3390/en16073265

Academic Editor: Dimitrios Kalderis

Received: 2 March 2023
Revised: 31 March 2023
Accepted: 4 April 2023
Published: 5 April 2023

1. Introduction

In South Korea, the level of returning excrement from livestock to farmland as nutrient resources for nitrogen and phosphorus has reached a limit [1]. The generation of phosphorus and nitrogen is 300,000 and 120,000 tons per year, respectively, with a load of 100,000 and 70,000 tons [2]. Additionally, seven of the nine provinces in the country are overloaded with nutrients by over 100%. Accordingly, the Ministry of Agriculture and Forestry promoted the introduction of the total nutrient quota system from 2016 to 2019, which was implemented in 2020 [3,4]. In livestock manure, the liquid portion of pork manure is maintained at an appropriate level through a governmental management system. In the case of cattle manure compost, no such system has been established, and it has been noted as a cause of environmental pollution problems, such as green algae [5]. As a result, several investigations are being conducted in the field of cattle manure energization.

The Ministry of Trade, Industry and Energy signed an agreement with three private power generation companies to stop using imported fuel pellets, or renewable energy certificates (RECs), to expand the utilization of unused domestic biomass [6]. Currently, 94% of the biomass pellets used by the three power generation companies rely on importation, which has the effect of creating a market value of about 240 billion won per year. Therefore, this study analyzed the feasibility of applying a process which produces solid fuels using cattle manure to target the pellet market. Furthermore, we analyzed the annual calorific value of imported wood pellets at three private companies and confirmed that 81% of the imported wood pellets can be substituted for the potential volumes of solid fuel produced from cattle manure [6–8].

The cattle manure is resistant to pulverization and accompanied by high transportation costs due to its high moisture and low energy density [9]. To produce solid fuel from cattle manure, three processes were selected: hydrothermal carbonization, torrefaction (mild pyrolysis), and carbonization (slow pyrolysis). The three processes convert biomass to a fuel that is more stable, has a higher energy density, friability, and grindability [10–12]. These results overcome the limitations of utilizing raw cattle manure in energy generation. The hydrothermal carbonization process is operated within the temperature range of 180–260 °C in a closed system with subcritical water [13]. In addition to having solid fuels as the final product, a liquid waste is produced which can be utilized as a substrate for anaerobic digestion. No pre-treatment is required for this process, but de-watering and drying are required at the end of the process [14–16]. The torrefaction and carbonization processes are performed under inert conditions at atmospheric pressure and are categorized according to temperature zones [17–19]. In terms of solid fuel production, the torrefaction process is operated at relatively low temperatures in the 200–320 °C range and produces some liquids and gases as byproducts in addition to solid fuels [20,21]. The torrefaction reaction progresses in the presence of limited devolatilization [22]. The aforementioned study on biomass torrefaction reported that a relatively high temperature and short residence time was more effective in enhancing the torrefied char's heating value [23]. Both processes were conducted after the drying pre-treatment process of the manure. The moisture content of feedstock should be less than 30% [24]. Additionally, for the efficiency of ignition and energy use, cooling is required after the production of solid fuels. On the other hand, the carbonization is characterized by a relatively high temperature range compared with torrefaction, around 400 °C (generally between 300 and 900 °C) with a slow heating rate, typically below 10 °C/min [25]. The process produces syn-gas, and bio-oils in addition to solid fuels known as biochar. Other studies have shown that the carbon in the final biochar increases with increasing pyrolysis temperatures [26,27]. Meanwhile, the oxygen and hydrogen content decrease. Biochars characteristically have a higher proportion of aromatic C, and condensed aromatic structures [28].

In this study, the hydrochar, torrefied char, and biochars of cattle manure were produced by three different carbonization processes. The physicochemical characteristics of hydrochar, torrefied char, and biochars were analyzed by proximate analysis, ultimate analysis, and heating values. The quality of hydrochar, torrefied char, and biochars were investigated by their fuel ratio, van Krevelen diagram, ash composition, and thermogravimetric analyses. The properties of hydrochar, torrefied char, and biochars that originated from cattle manure were used by applying the basic data on a combustion system and help determine a suitable fuel. The fundamental data in this paper are attributed to the feasibility analysis of different carbonization processes using cattle manure for the construction of a demonstration plant.

2. Materials and Methods

2.1. Cattle Manure

The cattle manure used in this study was obtained from a ranch in Icheon-si, South Korea, as shown in Figure 1. The results of the characterization, including moisture content, proximate analysis, elemental analysis, and calorific value, are listed in Table 1. The moisture content was found to be 66.05%, and the proximate analysis confirmed that the ash content was 20% or more in a dried condition, which is higher than the quality standard for livestock manure solid fuels in South Korea [29]. The elemental analysis also showed a high percentage of carbon and oxygen, 30% or more and 20% or more, respectively. The calorific value was found as an average of 12.55 MJ/kg in a dried condition. According to the Ministry of Environment's notification on the installation of solid fuel facilities for livestock manure, a moisture content of 20% or less was provided as the standard [29]. When a low calorific value was converted, it was confirmed that all of them were below 12.55 MJ/kg. Therefore, a process to upgrade cattle manure as a solid fuel is required.

(**a**) (**b**)

Figure 1. Sampling site (**a**) and collecting procedure (**b**) for cattle manure in Icheon-si, South Korea.

Table 1. The characteristic properties of cattle manure.

Properties	Cattle Manure
Moisture (wt. %, ar [1])	66.05
Proximate analysis (wt. %, db [2])	
Volatile matter	56.17
Fixed carbon	16.34
Ash	27.49
Ultimate analysis (wt. %, db [2])	
Carbon	36.19
Hydrogen	4.36
Oxygen	29.12
Nitrogen	1.87
Sulfur	0.97
Calorific analysis (MJ/kg, db [2])	
Lower heating value	12.93

[1] as received, [2] on dry basis.

2.2. Hydrothermal Carbonization

Experiments were performed using a 3 L lab-scale reactor. The hydrothermal carbonization reaction was carried out by combining 1 Kg of cattle manure with 100 g of distilled water, corresponding to a 10 wt.% of the feedstock. A certain amount of water was injected to offset the high viscosity of the sludge and to enhance the heat transfer effect through the steam. Stirring was performed with a constant torque at 250 rpm throughout the entire reaction process using a magnetic drive in order to supply uniform heat from the reactor's external heating jacket. Under fully sealed conditions, the reaction temperature conditions were set to 190 and 210 °C to achieve pressure conditions above 15–20 bar without additional gas injection, as previously reported [30,31]. The reaction time was 90 min, including 60 min for the temperature-rising step and 30 min for retention of the major reaction. After the reaction was terminated, the reaction mixture was allowed sufficient time to reach ambient pressure and room temperature. The hydrochar was separated from the liquid using 5 μm filter paper. The hydrochar was then dried at 105 °C for 24 h. The weight change and physical properties of the final reaction products were analyzed for characterization.

2.3. Torrefaction and Carbonization

For the torrefaction and carbonization reactions, the cattle manure was dried at 105 °C for 24 h until a constant weight was reached, to exclude the effect of drying on mass flow. Each test was conducted under normal pressures with 250 g of dried cattle manure in a 1 L reactor. Nitrogen was purged until the oxygen concentration in the reactor was less than or equal to 1%, and was continually monitored by a detector. Nitrogen was continuously added at a flow rate of 20 mL/min to maintain inert conditions. Temperature ranges were selected for the torrefaction and carbonization processes based on previous studies [32–35]. With an electric heater, the temperature was raised to 250 and 300 °C for the torrefaction process and 400 and 450 °C for the carbonization process for 1 h, and then the set temperature was maintained for 30 min. Additionally, the samples were stirred at a speed of 50 rpm to improve the efficient transfer of convective heat supplied from the reactor's walls by electric heaters. After temperature elevation and temperature hold was complete, and the samples were cooled down to room temperature. Finally, the weight change and physical properties of the torrefaction and carbonized samples were analyzed.

2.4. Mass and Energy Yield

The mass yield was expressed as a percentage of the dry weight of hydrochar, torrefied char, and biochar produced by the three processes based on the weight of cattle manure dried at 105 °C for 24 h, as shown in Equation (1).

$$\text{Mass yield} = \frac{\text{mass of dried biochar}}{\text{mass of dried raw material}} \times 100 \tag{1}$$

The energy densification ratio was the calorific value of the hydrochar, torrefied char, and biochar divided by the calorific value of the feedstock, as shown in Equation (2).

$$\text{Energy densification ratio} = \frac{\text{LHV of char via carbonization processes}}{\text{LHV of raw material}} \tag{2}$$

The energy yield, which represents the evaluated energy retained in solid fuels compared with that of the cattle manure [36], was the mass yield times the energy densification ratio, as expressed in Equation (3). Energy yield was utilized as an important performance indicator to compare the energy potential of hydrochar, torrefied char, and biochar produced in each process.

$$\text{Enegy yeild} = \text{mass yield } \times \text{energy densification ratio} \tag{3}$$

2.5. Thermogravimetric Analysis for Pyrolysis Behavior

The thermogravimetric analyses of cattle manure, hydrochar, torrefied char, and biochar were performed in a thermobalance NETZSCH (STA 449 F5) under non-isothermal conditions. A total of about 10 mg of whole dried samples was placed in an alumina crucible. Runs were performed between 100 and 700 °C at a heating rate of 10 °C/min under 100 mL/min of nitrogen. The conversion (α) of the sample in the overall pyrolysis process can be calculated as follows:

$$\alpha = \frac{W_0 - W}{W_0 - W_\infty} \tag{4}$$

where W_0, W, and W_∞ represent the instantaneous, initial, and final weights of the sample in the pyrolysis process, respectively.

3. Results

3.1. Comparison of the Properties of the Cattle Manure, Hydrochar, Torrefied Char, and Biochar

Table 2 summarizes the physicochemical properties of hydrochar produced from hydrothermal carbonization (CM-HTC), torrefied chars by torrefaction (CM-TF), and biochars via carbonization (CM-CB). It was found that volatile matter decreased from 56.17% in dry cattle manure (CM) to 11.49–51.37% in the hydrochar, torrefied char, and biochar produced from all carbonization processes, and it decreased in the order of hydrothermal carbonization, torrefaction, and carbonization. Fixed carbon was found to be within the range from 18.43 to 35.35% for all processes compared with 16.34% in cattle manure. It had a maximum increase in the order of hydrothermal, torrefaction, and carbonized by 31.09, 77.93, and 116.91%, respectively, compared with maximum in the raw material. The increase in fixed carbon correlates with the rise in aromatic carbon, which improves fuel quality [37]. Therefore, the rise in fixed carbon involves an increase in the heating value of char [38]. Whereas the reduction in elemental carbon and the heating value from 35.19% to 35.35–35.53%, and from 12.93 MJ/kg to 12.85–12.59 MJ/kg, respectively, was observed from the carbonization process. The reduction signifies a drop in the energy content of the char [39]. Ash content was found to increase from 30.20 to 52.06% compared with 27.49% in the raw material. An increase in the ash content was related to the amplification of the mineral concentration for the release of volatiles from the raw material during the carbonization processes. A rise in the mineral concentration leads to reduction in fuel qualities [38]. Additionally, a preceding study reported that dehydrogenation attributes to a reduction in the heating values at higher temperatures (above 450 °C) [40]. Dehydrogenation ingenerates char with a high percentage of inorganic materials. Thus, the elemental carbon and heating values of biochar produced by carbonization decreased compared with cattle manure.

Table 2. Proximate, ultimate, and calorific analysis of the feedstock, hydrochar, torrefied char, and biochar samples.

Descriptions	**CM (Raw)**	**CM-HTC (190 °C)**	**CM-HTC (210 °C)**	**CM-TF (250 °C)**	**CM-TF (300 °C)**	**CM-CB (400 °C)**	**CM-CB (450 °C)**
Proximate analysis (wt.%, d.b. [1])							
Volatiles	56.17	46.37	38.04	35.59	26.56	12.50	11.49
Fixed carbon	16.34	23.43	29.42	25.00	29.08	33.94	35.45
Ash	27.49	30.20	32.54	39.40	44.36	53.56	53.06
Ultimate analysis (wt.%, db. [1])							
Carbon	36.19	37.52	41.13	37.6	37.97	35.35	35.53
Hydrogen	4.36	3.88	4.46	3.13	2.67	1.75	1.41
Oxygen	29.12	20.7	18.56	16.87	12.21	6.93	7.77
Nitrogen	1.87	2.57	2.8	2.08	1.84	1.51	1.27
Sulfur	0.97	0.52	0.71	0.92	0.95	0.9	0.96
Calorific value (MJ/kg, d.b. [1])							
LHV	12.93	13.35	15.23	14.77	13.77	12.59	12.85

[1] A dry basis.

Through proximate analysis, we estimated the fuel ratio that can be expressed as fixed carbon to volatiles and summarized it as shown in Figure 2. The fuel ratio is used as an indicator of coal quality, with a high volatile fraction being conducive to the ignition behavior of the fuel in a combustor, while high fixed carbon is conducive to stable combustion [41,42]. Low fuel ratios result in a high ignition behavior, which causes spontaneous ignition during storage of the fuels. The high fuel ratios make ignition difficult, but they help maintaining a stable combustion process. The condition of the fuel ratio that maintains stable combustion is known to be in the range of 0.9 to 1.5 [43]. The fuel ratio for hydrochar, torrefied char, and biochar produced from torrefaction was found to be within 0.7–1.09, indicating stable combustion conditions. However, the ash content was found to be somewhat higher, ranging from 39.40 to 44.36%. In the case of the hydrothermal carbonization process, the initial ignition was considered smooth with a fuel ratio of 0.51–0.77, but a slightly higher process temperature was required for stable combustion. The ash content was 30–32.54%, which is considered to satisfy the conditions for stable combustion. The fuel ratio for the carbonization process showed the highest value of 2.71–3.08, indicating some difficulty in the initial ignition, but stable combustion is possible. However, the ash content was the highest, ranging from 53.06 to 53.56%.

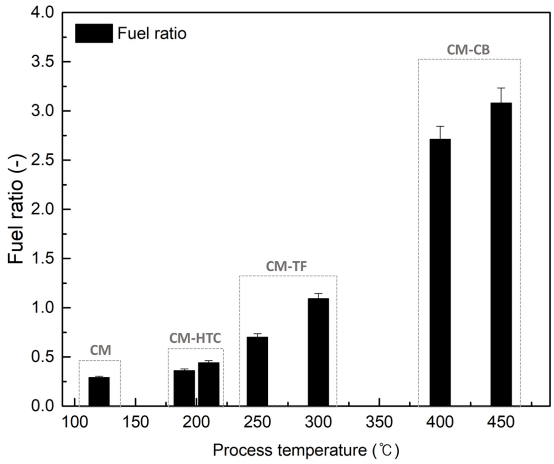

Figure 2. The fuel ratio of the cattle manure, hydrochar, torrefied char, and biochar.

Figure 3 presents the extent of the carbonization of hydrochar, torrefied char, and biochar's solid content in the raw material on the basis of cattle manure utilizing the van Krevelen diagram. The solid content produced by the three different carbonization processes exhibited an obvious drop in the H/C and O/C ratios because of the COOH functional group and H_2O leaving via dehydration and decarboxylation compared with that of cattle manure [44–46]. The low H/C and O/C ratios indicate the presence of more condensed structures [47,48].

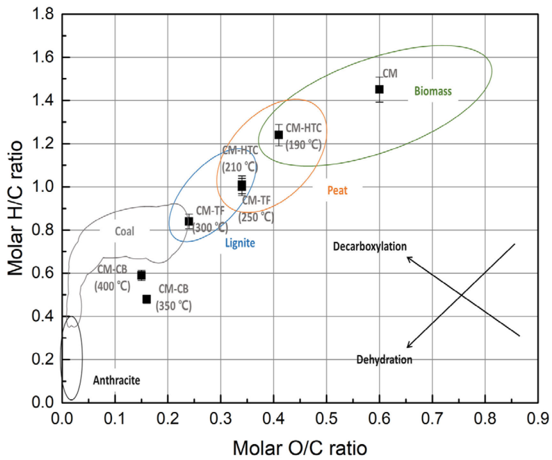

Figure 3. The van Krevelen diagram of the cattle manure, hydrochars, torrefied chars, and biochars.

The energy densification ratio and energy yield for the three carbonization processes are shown in Figure 4. For hydrothermal and carbonization processes, the energy densification ratio increased as the reaction temperature increased, but the ratio decreased for torrefaction. Similar to previous studies, we found that severe torrefaction at 300 °C reduced the energy density and is therefore not suitable for cattle manure [33]. The highest energy densification ratio of 1.18 was found for the hydrothermal carbonization process at 210 °C, and a similar value of 1.14 was found for the torrefaction process at 250 °C. For the carbonization process, on the other hand, the energy densification ratio was found to be the lowest at 0.97–0.99. On the other hand, the energy yield considering the calorific value and mass yield showed the highest value of 78.52% in the torrefaction process under 250 °C, and a similar value of 77.56% was found in the hydrothermal carbonization at 210 °C. On the other hand, the energy yield for the carbonization process was found to be 49.69–50.94%, which is considered unfavorable compared with other processes in terms of solid fuel production. The behavior of the three carbonizations is very similar to the findings of previous studies [31,33,34].

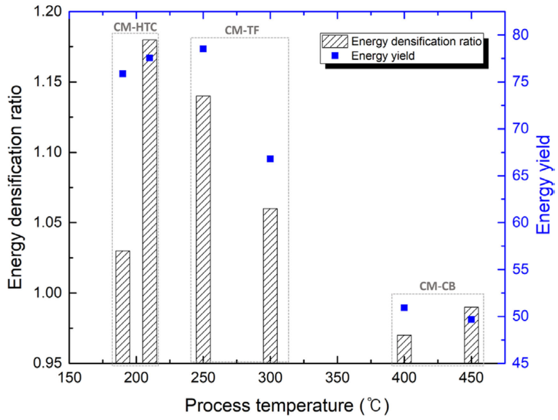

Figure 4. Energy densification ratio and energy yield of the hydrochar, torrefied char, and biochar derived from cattle manure.

3.2. Characteristics of Ash in Cattle Manure, Hydrochar, Torrefied Char, and Biochar

The ash content, a non-combustible material, is one of the quality standards required for hydrochar, torrefied char, and biochar as a solid fuel [49]. Ashes do not burn in the furnace or boiler, and some fine particles move with the flow of the flue gas. When the temperature of the combustion chamber is higher than the melting point of the ash, due to the high flue gas temperature, the ash particles hit the water pipe wall in a molten state and rapidly cool down, agglomerate, adhere, and accumulate on the water pipe wall. This phenomenon is called slagging, and it is called fouling when the ash passes through the convective heating surface with the combustion gases at a relatively low temperature, condenses and adheres to the superheater or reheater, and solidifies [50]. This ash residue reduces heat transfer in the heat exchanger tubes, resulting in a low boiler efficiency and capacity, obstructed flow of internal fluids, mechanical damage, and corrosion. This may even require a shutdown, resulting in energy and economic losses [51].

Various indices have been reported for predicting coal ash adhesion based on basic composition analysis and laboratory-scale experimental data, and are summarized in Table 3 [52–54]. The elemental composition of samples for ash in an oxidized atmosphere were obtained by X-ray florescence (XRF) analysis.

Table 3. Slagging and fouling indices.

Index	Slagging and Fouling Indices			
	Low	**Medium**	**High**	**Extremely High**
SiO_2 (%)	<20	20~25	>25	-
Cl (%)	<0.2	0.2~0.3	0.3~0.5	>0.5
B/A ratio	<0.5	0.5~1	1~1.75	>1.75

Silica is the dominant element in slag and has been confirmed to form a sticky substance in slagging [55,56]. The content of silica in the fuel ash was found to correlate with the degree of slag formation in the burner. As shown in Figure 5, the frequency of slagging, predicted by utilizing SiO_2 in the ash of the generated cattle manure-based hydrochar, torrefied char, and biochar in the raw material, was considered as low. Compared with the raw material, a slight improvement in SiO_2 was observed in the carbonization process except for the hydrothermal carbonization process at 210 °C. It was found that SiO_2 decreased with increasing reaction temperature in the hydrothermal and carbonization processes, but it increased in torrefaction. Previous studies have reported the removal of silicon during hydrothermal carbonization in a specific range from 200 to 230 °C [57,58]. The subcritical conditions of water during the hydrothermal carbonization process characterize a lower density and viscosity than that of water at normal conditions [59]. In these conditions the removal of simple ionic salts in the cattle manure matrix can be enhanced. The increase in the dielectric content, ionic dissociation constant, and decrease in pH of subcritical water are attributable to the removal of ionic-bonded inorganics via ion exchange and the dissolving of inorganic salts [60–62]. Accordingly, a pronounced decrease in hydrochar produced at 210 °C was observed.

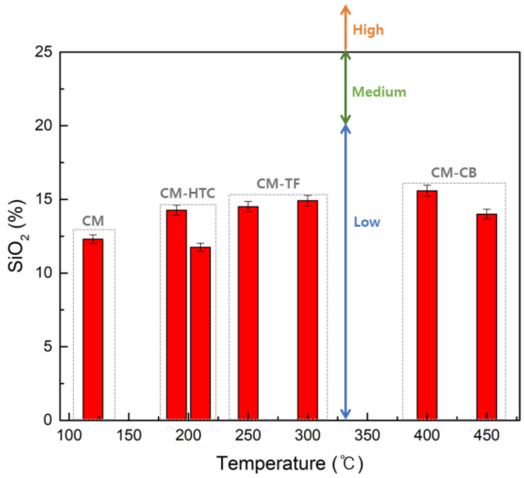

Figure 5. Silicon dioxide content in the cattle manure, hydrochar, torrefied char, and biochar.

Chlorine (Cl) plays a role for the reaction of potassium and silica, resulting in the formation of ash fusibility and slag at the operating temperatures of boilers, ranging from 800 to 900 °C [63,64]. Therefore, Cl can be an indicator of the slagging and fouling tendencies in biomass fuels [65,66]. The content of Cl in the ash of the hydrochars, torrefied chars, and biochars produced in this study is shown in Figure 6. The Cl content for both dry cattle manure and the hydrochars, torrefied chars, and biochars was 0.5% or more, categorizing into the extremely high fouling and slagging tendencies. The Cl fraction was analyzed as 7.34% for cattle manure and it increased to 7.54–7.84% for torrefied chars and carbonized biochars, higher than the raw material. On the other hand, hydrochar had a Cl content in the range of 2.59 to 2.77%, representing a 64.69% reduction compared with the dry process. This is due to two main mechanisms in the hydrothermal carbonization process: elimination and substitution reactions [67]. Removal of HCl and substitution of Cl can convert soluble organic chlorine to inorganic chlorine. Thus, the removal of chlorine from the raw material is achieved [68,69]. In particular, the degradation of lignocellulosic components promotes de-chlorination reactions. Lignin, hemicellulose, and cellulose provide many free -OH bonds [70], promoting the substitution of Cl [71].

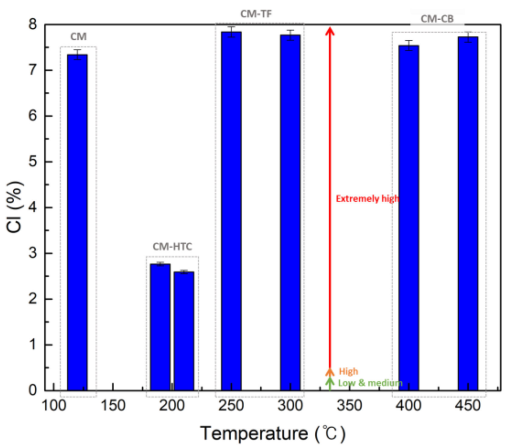

Figure 6. Chlorine content in the cattle manure, hydrochar, torrefied char, and biochar.

There are basic components (i.e., Fe_2O_3, CaO, MgO, Na_2O, and K_2O) in the ash lower the melting temperature [72]. These groups are categorized as Group B. P_2O_5 is reported to lower the melting point in fly ash and was, accordingly, added to Group B [53,72]. The acidic components (i.e., SiO_2, Al_2O_3, and TiO_2) increase the melting point and are defined as Group A. The base-to-acid (B/A) mass ratio can be expressed by the equation below, and can predict the deposition behavior of ash [53,73,74].

$$B/A\ \text{ratio} = \frac{(Fe_2O_3 + CaO + MgO + Na_2O + K_2O + P_2O_5)}{(SiO_2 + Al_2O_3 + TiO_2)} \quad (5)$$

Figure 7 depicts the B/A ratio in the cattle manure and the hydrochars, torrefied chars, and biochars. For all samples, the maximum basic components were 70% higher than the acidic components in the ash. An additional process for the elimination of basic components in ash is required for stable combustion operation.

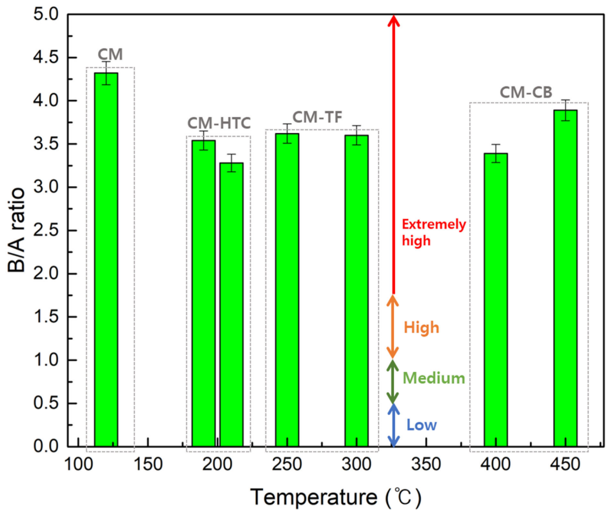

Figure 7. B/A ratio in the cattle manure, hydrochar, torrefied char, and biochar.

3.3. Thermogravimetric Analysis of the Cattle Manure, Hydrochar, Torrefied Char, and Biochars during Pyrolysis

Figures 8 and 9 exhibit the TG and DTG curves, respectively, for the cattle manure and the hydrochars, torrefied chars, and biochars in inert atmospheres. Table 4 summarizes the reaction indexes, comprising initial, maximum, final pyrolysis temperatures, maximum degradation rates, and residual fractions. The kinetics parameters and mass fractions were calculated according to the residual mass of the dried samples. The drying process was not included in this study. The main stages of thermal decomposition and the corresponding mass losses of the cattle manure and the hydrochars, torrefied chars, and biochars during the pyrolysis occurred over a wide temperature range. In addition, asymmetrical DTG curves were obtained, which primarily verified the use of heterogeneous materials. Examples of such materials include biomasses obtained between 178 and 696 °C through the decomposition of cattle manure, including general lignocellulosic biomass materials and extractives [75]. Thus, the main components of cattle manure comprise cellulose, hemicellulose, lignin, and partially undigested organic matter. Based on the mass loss profiles of the raw materials, hydrochars, torrefied chars, and biochars all exhibited different behaviors. In the raw material sample, the main weight loss occurred from 185 to 675 °C (approximately 53% of the total weight loss), and the maximum weight loss rate was 0.048 min^{-1} (approximately at 320 °C).

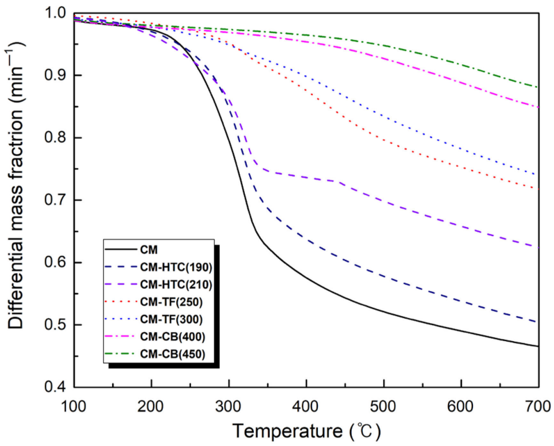

Figure 8. Experimental pyrolytic TG curves of the cattle manure, hydrochar, torrefied char, and biochar.

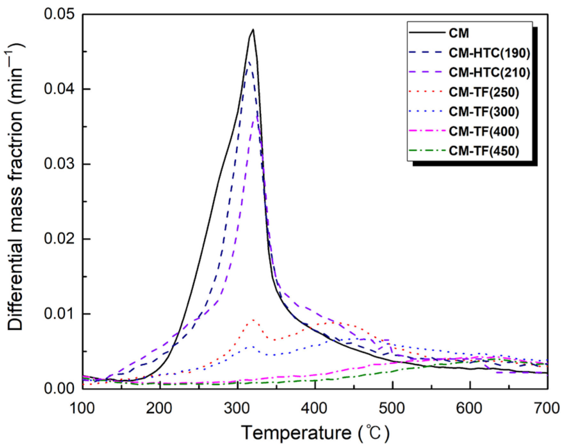

Figure 9. Experimental pyrolytic DTG curves of the cattle manure, hydrochar, torrefied char, and biochar.

Table 4. Characteristics of the cattle manure, hydrochar, torrefied char, and biochar during pyrolysis.

Sample	T_i (°C)	T_{pk} (°C)	T_f (°C)	R_{pk} (min^{-1})	M_f (g/g)
CM	185	320	675	4.80×10^{-2}	0.47
CM-HTC (190 °C)	140	315	675	4.38×10^{-2}	0.51
CM-HTC (210 °C)	135	335	675	3.64×10^{-2}	0.59
CM-TF (250 °C)	190	419	675	8.84×10^{-3}	0.72
CM-TF (300 °C)	200	460	675	6.71×10^{-3}	0.74
CM-CB (400 °C)	370	610	675	4.03×10^{-3}	0.85
CM-CB (450 °C)	450	635	680	4.02×10^{-3}	0.88

The main weight loss of the hydrochars was observed to start at approximately 135–140 °C, which is lower than that of the raw materials. As the temperature increased to 315–325 °C, fractional weight loss rates increased, achieving maximum values of 0.0364–0.0438 min^{-1}. For the torrefied chars, two visible peaks can be observed in the DTG curves corresponding to the maximum mass loss. The first peak corresponds to the degradation of cellulose at 309–310 °C, and the second relates to lignin at 419–460 °C. Such a tendency coincides with the findings of other studies [76]. The degradation of the biochars produced via carbonization occurs at temperatures of 370–450 °C, which may imply that most hemicellulose was decomposed.

The deduced data are conformable with the fixed carbon and char obtained through the proximate analyses in Table 1. With respect to the characteristics of solid fuels, hydrochars, torrefied chars, and biochars of the cattle manure exhibit the maximum weight loss. Further, the amount of volatile matter is lower than those associated with the raw materials during pyrolysis, and the maximum pyrolysis temperature shifted to the right as the temperature increased. This can be primarily attributed to the breaking of weak bonds and the subsequent coalification process resulting from a series of reactions during the different carbonization processes [77,78]. Based on the three carbonization processes considered in this study, the maximum weight loss rates and the amount of volatile matter decreased with the increasing reaction temperature.

4. Conclusions

The characteristics of hydrochar, torrefied char, and biochar derived from cattle manure were analyzed to ascertain the adequacy of different carbonization processes. The main focus concerned comparing the extent of solid fuel quality and energy densification.

For the three carbonization processes, with increasing temperature, the volatile content reduced, while the fixed carbon increased compared with the cattle manure. These results imply an improved fuel quality. For all processes, the fuel ratio increased, and the O/C and H/C ratios decreased. The findings also demonstrate the conversion of cattle manure into a coal-like solid fuel. The heating value increased for hydrochars and torrefied chars, while for biochars, it decreased, caused by an increase in the mineral concentration. Concerning energy densification and energy yield, the hydrothermal carbonization at 210 °C and torrefaction at 250 °C showed the highest values and were considered optimal processes for the efficient production of solid fuels derived from cattle manure.

The ash composition of hydrochars, torrefied chars, and biochars was analyzed to predict the slagging and fouling tendencies in the combustion process as solid fuels. With respect to the silica content, the hydrochars, torrefied chars, and biochars tended to have low slagging occurrences. Conversely, based on the Cl and B/A ratios, hydrochars, torrefied chars, and biochars were considered in this study to have high probabilities of slagging and fouling occurrences. Hence, eliminating chlorine and basic oxide in the ash is required for stable combustion operation in industrial boilers.

The pyrolysis behaviors of hydrochars, torrefied chars, and biochars were distinct via thermogravimetric analysis. The solid fuels of the cattle manure were improved by the different carbonization processes demonstrating that the maximum degradation and the amount of volatiles were lower than those of the cattle manure in the pyrolysis process. It can thus be concluded that chars produced by the three different carbonization processes have appropriate characteristics to be used for incineration and boiler operations.

Author Contributions: Conceptualization, E.S.; methodology, E.S. and Y.-M.Y.; validation, E.S. and H.K.; formal analysis, K.W.K. and E.S.; investigation, K.W.K., H.K. and E.S.; resources Y.-M.Y. and E.S.; data curation, H.K. and E.S.; writing—original draft preparation, E.S.; writing—review and editing, E.S.; supervision, H.K. and Y.-M.Y.; project administration, H.K. All authors have read and agreed to the published version of the manuscript.

Funding: This work was supported by the Korea Institute of Energy Technology Evaluation and Planning (KETEP) and the Ministry of Trade, Industry and Energy (MOTIE) of the Republic of Korea (No. 20183010092750).

Data Availability Statement: Not applicable.

Conflicts of Interest: The authors declare no conflict of interest. The funding agencies had no role in the design of the study; in the collection analyses, or interpretation of data; in the writing of the manuscript; or in the decision to publish the results.

References

1. Won, S.; You, B.G.; Ra, C. Investigation of Hanwoo manure management and estimation of nutrient loading coefficients on land application. *J. Anim. Sci. Technol.* **2015**, *57*, 20. [CrossRef]
2. Lee, J.H.; Yoon, Y.M. Comparison of nutrient balance and nutrient loading index for cultivated land nutrient management. *Korean J. Environ. Biol.* **2019**, *37*, 554–567. [CrossRef]

3. Korea Rural Economic Institute Report, Introduction Plan Research of Nutrition Balance and Load. Available online: https://scienceon.kisti.re.kr/srch/selectPORSrchReport.do?cn=TRKO201600011825 (accessed on 10 January 2023).
4. Korea Ministry of Environment, Press Release. Available online: http://www.me.go.kr/home/web/board/read.do?boardMasterId=1&boardId=1507030&menuId=10525 (accessed on 10 January 2023).
5. Kim, Y.; Ryoo, K.S. Study on the Morphological Change and Reduction Plan of Nitrogen and Phosphorous in Litter and Manure of Cow House. *J. Korean Chem. Soc.* **2021**, *65*, 249–253.
6. Korea Ministry of Trade, Industry and Energy, Press Release. Available online: http://www.motie.go.kr/motie/ne/presse/press2/bbs/bbsView.do?bbs_cd_n=81&cate_n=1&bbs_seq_n=164505 (accessed on 10 January 2023).
7. Korea Administrative Rule, Quality Standards of Timber and Timber Products. Available online: https://www.law.go.kr/LSW/admRulLsInfoP.do?admRulSeq=2100000190670 (accessed on 13 January 2023).
8. Korea Electric Power Statistics Information System, Statistical Data of Fuel Cost. Available online: https://epsis.kpx.or.kr/epsisnew/selectEkmaFucUpfChart.do?menuId=040100 (accessed on 13 January 2023).
9. Batidzirai, B.; Mignot, A.P.R.; Schakel, W.B.; Junginger, H.M.; Faaij, A.P.C. Biomass torrefaction technology: Techno-economic status and future prospects. *Energy* **2013**, *62*, 196–214. [CrossRef]
10. Sharma, H.B.; Panigrahi, S.; Dubey, B.K. Hydrothermal carbonization of yard waste for solid bio-fuel production: Study on combustion kinetic, energy properties, grindability and flowability of hydrochar. *Waste Manag.* **2019**, *91*, 108–119. [CrossRef]
11. Yu, S.; Park, J.; Kim, M.; Kim, H.; Ryu, C.; Lee, Y.; Yang, W.; Jeong, Y.G. Improving energy density and grindability of wood pellets by dry torrefaction. *Energy Fuels* **2019**, *33*, 8632–8639. [CrossRef]
12. Chen, W.H.; Lin, B.J.; Lin, Y.Y.; Chu, Y.S.; Ubando, A.T.; Show, P.L.; Ong, H.C.; Chang, J.S.; Ho, S.H.; Culaba, A.B.; et al. Progress in biomass torrefaction: Principles, applications and challenges. *Prog. Energy Combust. Sci.* **2021**, *82*, 100887. [CrossRef]
13. Davies, G.; El Sheikh, A.; Collett, C.; Yakub, I.; McGregor, J. *Catalytic Carbon Materials from Biomass*; Elsevier: Amsterdam, The Netherlands, 2021; pp. 161–195.
14. Goyal, H.B.; Seal, D.; Saxena, R.C. Bio-fuels from thermochemical conversion of renewable resources: A review. *Renew. Sustain. Energy Rev.* **2008**, *12*, 504–517. [CrossRef]
15. Manyà, J.J. Pyrolysis for biochar purposes: A review to establish current knowledge gaps and research needs. *Environ. Sci Technol.* **2012**, *46*, 7939–7954. [CrossRef] [PubMed]
16. Mosier, N.; Wyman, C.; Dale, B.; Elander, R.; Lee, Y.; Holtzapple, M.; Ladisch, M. Features of promising technologies for pretreatment of lignocellulosic biomass. *Bioresour. Technol.* **2005**, *96*, 673–686. [CrossRef]
17. Fokaides, P.A. *Energy Recovery Alternatives for the Sustainable Management of Olive Oil Industry*; Academic Press: Cambridge, MA, USA, 2017; pp. 79–96.
18. Guo, M.; Song, W.; Buhain, J. Bioenergy and biofuels: History, status, and perspective. *Renew. Sustain. Energy Rev.* **2015**, *42*, 712–725. [CrossRef]
19. Kambo, H.S.; Dutta, A. A comparative review of biochar and hydrochar in terms of production, physico-chemical properties and applications. *Renew. Sustain. Energy Rev.* **2015**, *45*, 359–378. [CrossRef]
20. Kusch-Brandt, S.; Mumme, J.; Nashalian, O.; Girotto, F.; Lavagnolo, M.C.; Udenigwe, C. *Valorization of Residues from Beverage Production*; Woodhead Publication: New Delhi, India, 2019; pp. 451–494.
21. Li, S.X.; Chen, C.Z.; Li, M.F.; Xiao, X. Torrefaction of corncob to produce charcoal under nitrogen and carbon dioxide atmospheres. *Bioresour. Technol.* **2018**, *249*, 348–353. [CrossRef]
22. Ren, X.; Sun, R.; Meng, X.; Vorobiev, N.; Schiemann, M.; Levendis, Y.A. Carbon, sulfur and nitrogen oxide emissions from combustion of pulverized raw and torrefied biomass. *Fuel* **2017**, *188*, 310–323. [CrossRef]
23. Chen, W.H.; Huang, M.Y.; Chang, J.S.; Chen, C.Y.; Lee, W.J. An energy analysis of torrefaction for upgrading microalga residue as a solid fuel. *Bioresour. Technol.* **2015**, *185*, 285–293. [CrossRef]
24. Cai, N.; Zhang, H.; Nie, J.; Deng, Y.; Baeyens, J. Biochar from biomass slow pyrolysis. In *IOP Conference Series: Earth and Environmental Science*; IOP Publishing: Bristol, UK, 2020; Volume 586, p. 012001.
25. Zhang, Y.; Cui, Y.; Chen, P.; Liu, S.; Zhou, N.; Ding, K.; Fan, L.; Peng, P.; Min, M.; Cheng, Y.; et al. *Gasification Technologies and Their Energy Potentials*; Elsevier: Amsterdam, The Netherlands, 2019; pp. 193–206.
26. Sizirici, B.; Fseha, Y.H.; Yildiz, I.; Delclos, T.; Khaleel, A. The effect of pyrolysis temperature and feedstock on date palm waste derived biochar to remove single and multi-metals in aqueous solutions. *Sustain. Environ. Res.* **2021**, *31*, 1–16. [CrossRef]
27. Chatterjee, R.; Sajjadi, B.; Chen, W.Y.; Mattern, D.L.; Hammer, N.; Raman, V.; Dorris, A. Effect of pyrolysis temperature on physicochemical properties and acoustic-based amination of biochar for efficient CO2 adsorption. *Front. Energy Res.* **2020**, *8*, 85. [CrossRef]
28. Schmidt, M.W.; Noack, A.G. Black carbon in soils and sediments: Analysis, distribution, implications, and current challenges. *Glob. Biogeochem. Cycles* **2000**, *14*, 777–793. [CrossRef]
29. Korea Administrative Rule, Announcement for Installation of Solid Fuel Production Facilities Derived from Livestock Excretions. Available online: https://www.law.go.kr/LSW/admRulLsInfoP.do?admRulSeq=2100000139032 (accessed on 15 January 2023).
30. Toufiq Reza, M.; Freitas, A.; Yang, X.; Hiibel, S.; Lin, H.; Coronella, C.J. Hydrothermal carbonization (HTC) of cow manure: Carbon and nitrogen distributions in HTC products. *Environ. Prog. Sustain. Energy* **2016**, *35*, 1002–1011. [CrossRef]
31. Marin-Batista, J.D.; Villamil, J.A.; Qaramaleki, S.V.; Coronella, C.J.; Mohedano, A.F.; de La Rubia, M.A. Energy valorization of cow manure by hydrothermal carbonization and anaerobic digestion. *Renew. Energy* **2020**, *160*, 623–632. [CrossRef]

32. Sitty, N.S.B.; Pyohei, Y.; Iw, A.K. Preliminary Study of Dairy Manure Torrefaction for Biochar Production. In Proceedings of the ISER 9th International Conference, Berlin, Germany, 30 October 2015.
33. Itoh, T.; Iwabuchi, K.; Maemoku, N.; Chen, S.; Taniguro, K. Role of ambient pressure in self-heating torrefaction of dairy cattle manure. *PLoS ONE* **2020**, *15*, e0233027. [CrossRef] [PubMed]
34. Tsai, W.T.; Huang, P.C.; Lin, Y.Q. Characterization of biochars produced from dairy manure at high pyrolysis temperatures. *Agronomy* **2019**, *9*, 634. [CrossRef]
35. Atienza-Martínez, M.; Ábrego, J.; Gea, G.; Marías, F. Pyrolysis of dairy cattle manure: Evolution of char characteristics. *J. Anal. Appl. Pyrolysis* **2020**, *145*, 104724. [CrossRef]
36. Li, X.; Li, M.F.; Bian, J.; Wang, B.; Xu, J.K.; Sun, R.C. Hydrothermal carbonization of bamboo in an oxalic acid solution: Effects of acid concentration and retention time on the characteristics of products. *RSC Adv.* **2015**, *5*, 77147–77153. [CrossRef]
37. Wu, W.; Yang, M.; Feng, Q.; McGrouther, K.; Wang, H.; Lu, H.; Chen, Y. Chemical characterization of rice straw-derived biochar for soil amendment. *Biomass Bioenergy* **2012**, *47*, 268–276. [CrossRef]
38. Rafiq, M.K.; Bachmann, R.T.; Rafiq, M.T.; Shang, Z.; Joseph, S.; Long, R. Influence of pyrolysis temperature on physico-chemical properties of corn stover (*Zea mays* L.) biochar and feasibility for carbon capture and energy balance. *PLoS ONE* **2016**, *11*, e0156894. [CrossRef]
39. Soka, O.; Oyekola, O. A feasibility assessment of the production of char using the slow pyrolysis process. *Heliyon* **2020**, *6*, e04346. [CrossRef]
40. Mundike, J.; Collard, F.X.; Görgens, J.F. Pyrolysis of Lantana camara and Mimosa pigra: Influences of temperature, other process parameters and incondensable gas evolution on char yield and higher heating value. *Bioresour. Technol.* **2017**, *243*, 284–293. [CrossRef]
41. Aich, S.; Nandi, B.K.; Bhattacharya, S. Utilization of sal leaves and sal leaves char to improve the combustion performance of reject coal. *Energy Sources Part A Recover. Util. Environ. Eff.* **2019**, *41*, 2299–2312. [CrossRef]
42. Liu, X.; Chen, M.; Wei, Y. Kinetics based on two-stage scheme for co-combustion of herbaceous biomass and bituminous coal. *Fuel* **2015**, *143*, 577–585. [CrossRef]
43. Aich, S.; Behera, D.; Nandi, B.K.; Bhattacharya, S. Relationship between proximate analysis parameters and combustion behaviour of high ash Indian coal. *Int. J. Coal Sci. Technol.* **2020**, *7*, 766–777. [CrossRef]
44. Gao, P.; Zhou, Y.; Meng, F.; Zhang, Y.; Liu, Z.; Zhang, W.; Xue, G. Preparation and characterization of hydrochar from waste eucalyptus bark by hydrothermal carbonization. *Energy* **2016**, *97*, 238–245. [CrossRef]
45. Fan, F.; Zheng, Y.; Huang, Y.; Lu, Y.; Wang, Z.; Chen, B.; Zheng, Z. Preparation and characterization of biochars from waste Camellia oleifera shells by different thermochemical processes. *Energy Fuels* **2017**, *31*, 8146–8151. [CrossRef]
46. Zhao, Y.; Su, R.; Zhang, W.; Yao, G.L.; Chen, J. Antibacterial activity of tea saponin from Camellia oleifera shell by novel extraction method. *Ind. Crops Prod.* **2020**, *153*, 112604. [CrossRef]
47. Schimmelpfennig, S.; Glaser, B. One step forward toward characterization: Some important material properties to distinguish biochars. *J. Environ. Qual.* **2012**, *41*, 1001–1013. [CrossRef] [PubMed]
48. Chun, Y.; Sheng, G.; Chiou, C.T.; Xing, B. Compositions and sorptive properties of crop residue-derived chars. *Environ. Sci. Technol.* **2004**, *38*, 4649–4655. [CrossRef] [PubMed]
49. Zevenhoven, M.; Yrjas, P.; Skrifvars, B.J.; Hupa, M. Characterization of ash-forming matter in various solid fuels by selective leaching and its implications for fluidized-bed combustion. *Energy Fuels* **2012**, *26*, 6366–6386. [CrossRef]
50. Moskal, T.; Scott, S. *Economic Consequences of Boiler Cheanning Effectiveness*; Technical Publication Report No. DPTP-98-1; Diamond Power International: Lancaster, OH, USA, 1998.
51. Singer, J.G. *Combustion, Fossil Power Systems: A Reference Book on Fuel Burning and Steam Generation*; Combustion Engineering Power Systems Group: Columbia, MD, USA, 1981.
52. Öhman, M.; Nordin, A.; Hedman, H.; Jirjis, R. Reasons for slagging during stemwood pellet combustion and some measures for prevention. *Biomass Bioenergy* **2004**, *27*, 597–605. [CrossRef]
53. Masiá, A.T.; Buhre, B.J.P.; Gupta, R.P.; Wall, T.F. Characterising ash of biomass and waste. *Fuel Process. Technol.* **2007**, *88*, 1071–1081. [CrossRef]
54. Munir, S.; Nimmo, W.; Gibbs, B.M. The effect of air staged, co-combustion of pulverised coal and biomass blends on NOx emissions and combustion efficiency. *Fuel* **2011**, *90*, 126–135. [CrossRef]
55. Öhman, M.; Boman, C.; Hedman, H.; Nordin, A.; Boström, D. Slagging tendencies of wood pellet ash during combustion in residential pellet burners. *Biomass Bioenergy* **2004**, *27*, 585–596. [CrossRef]
56. Gilbe, C.; Öhman, M.; Lindström, E.; Boström, D.; Backman, R.; Samuelsson, R.; Burvall, J. Slagging characteristics during residential combustion of biomass pellets. *Energy Fuels* **2008**, *22*, 3536–3543. [CrossRef]
57. Stirling, R.J.; Snape, C.E.; Meredith, W. The impact of hydrothermal carbonisation on the char reactivity of biomass. *Fuel Process. Technol.* **2018**, *177*, 152–158. [CrossRef]
58. Smith, A.M.; Singh, S.; Ross, A.B. Fate of inorganic material during hydrothermal carbonisation of biomass: Influence of feedstock on combustion behaviour of hydrochar. *Fuel* **2016**, *169*, 135–145. [CrossRef]
59. Wagner, W.; Pruß, A. The IAPWS formulation 1995 for the thermodynamic properties of ordinary water substance for general and scientific use. *J. Phys. Chem. Ref. Data* **2002**, *31*, 387–535. [CrossRef]
60. Archer, D.G.; Wang, P. The dielectric constant of water and Debye-Hückel limiting law slopes. *J. Phys. Chem. Ref. Data* **1990**, *19*, 371–411. [CrossRef]

61. Bandura, A.V.; Lvov, S.N. The ionization constant of water over wide ranges of temperature and density. *J. Phys. Chem. Ref. Data* **2006**, *35*, 15–30. [CrossRef]
62. Kruse, A.; Funke, A.; Titirici, M.M. Hydrothermal conversion of biomass to fuels and energetic materials. *Curr. Opin. Chem. Biol.* **2013**, *17*, 515–521. [CrossRef]
63. Jenkins, B.M.; Bakker, R.R.; Wei, J.B. On the properties of washed straw. *Biomass Bioenergy* **1996**, *10*, 177–200. [CrossRef]
64. Llorente, M.F.; Laplaza, J.M.; Cuadrado, R.E.; García, J.C. Ash behaviour of lignocellulosic biomass in bubbling fluidised bed combustion. *Fuel* **2006**, *85*, 1157–1165. [CrossRef]
65. Miles, T.R.; Miles, T.R., Jr.; Baxter, L.L.; Bryers, R.W.; Jenkins, B.M.; Oden, L.L. Boiler deposits from firing biomass fuels. *Biomass Bioenergy* **1996**, *10*, 125–138. [CrossRef]
66. Nutalapati, D.; Gupta, R.; Moghtaderi, B.; Wall, T.F. Assessing slagging and fouling during biomass combustion: A thermodynamic approach allowing for alkali/ash reactions. *Fuel Process. Technol.* **2007**, *88*, 1044–1052. [CrossRef]
67. Shen, Y. Dechlorination of poly (vinyl chloride) wastes via hydrothermal carbonization with lignin for clean solid fuel production. *Ind. Eng. Chem. Res.* **2016**, *55*, 11638–11644. [CrossRef]
68. Huang, N.; Zhao, P.; Ghosh, S.; Fedyukhin, A. Co-hydrothermal carbonization of polyvinyl chloride and moist biomass to remove chlorine and inorganics for clean fuel production. *Appl. Energy* **2019**, *240*, 882–892. [CrossRef]
69. Poerschmann, J.; Weiner, B.; Woszidlo, S.; Koehler, R.; Kopinke, F.D. Hydrothermal carbonization of poly (vinyl chloride). *Chemosphere* **2015**, *119*, 682–689. [CrossRef]
70. Tekin, K.; Karagöz, S.; Bektaş, S. A review of hydrothermal biomass processing. *Renew. Sustain. Energy Rev.* **2014**, *40*, 673–687. [CrossRef]
71. Yao, Z.; Ma, X. Characteristics of co-hydrothermal carbonization on polyvinyl chloride wastes with bamboo. *Bioresour. Technol.* **2018**, *247*, 302–309. [CrossRef]
72. Munir, S.; Nimmo, W.; Gibbs, B.M. Potential slagging and fouling problems associated with biomass-coal blends in coal-fired boilers. *J. Pak. Inst. Chem. Eng* **2010**, *38*, 1–11.
73. Pronobis, M. Evaluation of the influence of biomass co-combustion on boiler furnace slagging by means of fusibility correlations. *Biomass Bioenergy* **2005**, *28*, 375–383. [CrossRef]
74. Vamvuka, D.; Zografos, D. Predicting the behaviour of ash from agricultural wastes during combustion. *Fuel* **2004**, *83*, 2051–2057. [CrossRef]
75. Yuan, X.; He, T.; Cao, H.; Yuan, Q. Cattle manure pyrolysis process: Kinetic and thermodynamic analysis with isoconver-sional methods. *Renew. Energy* **2017**, *107*, 489–496. [CrossRef]
76. Mukherjee, A.; Okolie, J.A.; Niu, C.; Dalai, A.K. Experimental and modeling studies of torrefaction of spent coffee grounds and coffee husk: Effects on surface chemistry and carbon dioxide capture performance. *ACS Omega* **2021**, *7*, 638–653. [CrossRef]
77. Keiller, B.G.; Muhlack, R.; Burton, R.A.; van Eyk, P.J. Biochemical Compositional Analysis and Kinetic Modeling of Hy-drothermal Carbonization of Australian Saltbush. *Energy Fuels* **2019**, *33*, 12469–12479. [CrossRef]
78. Lucian, M.; Volpe, M.; Fiori, L. Hydrothermal carbonization kinetics of lignocellulosic agro-wastes: Experimental data and modeling. *Energies* **2019**, *12*, 516. [CrossRef]